analytical chemistry

Article

pubs.acs.org/ac

"Replica-Extraction-Transfer" Nanostructure-Initiator Mass Spectrometry Imaging of Acoustically Printed Bacteria

Katherine B. Louie,[†] Benjamin P. Bowen,[†] Xiaoliang Cheng,[†] James E. Berleman,[†] Romy Chakraborty,[†] Adam Deutschbauer,[†] Adam Arkin,[†,‡] and Trent R. Northen*[,†]

[†]Lawrence Berkeley National Laboratory, Berkeley, CA 94720, U.S.A.

[‡]UC Berkeley, Berkeley, CA 94720, U.S.A.

Supporting Information

ABSTRACT: Traditionally, microbes are studied under controlled laboratory conditions as isolates in planktonic culture. However, this is a vast extrapolation from their natural state; development of new techniques is required to decipher the largely unknown world of microbial chemical interactions in more realistic environments. The field of mass spectrometry imaging has made significant progress in localizing metabolites in and around bacterial colonies, primarily by using MALDI and ESI-based techniques that interrogate the top surface of the sample. Unfortunately, surface-based laser-desorption techniques, such as nanostructure-initiator mass spectrometry (NIMS), which has advantages in detection of small metabolite compounds and low background, has not been suitable for direct microbe imaging because desorption/ionization occurs on the bottom of the sample. Here, we describe a "replica-extraction-transfer" (REX) technique that overcomes this barrier by transferring biomolecules from agar cultures of spatially arrayed bacterial colonies onto NIMS surfaces; further, we demonstrate that acoustic printing of bacteria can be used to create complex colony geometries to probe microbial interactions with NIMS imaging. REX uses a solvent-laden semisolid (e.g., gel) to first extract metabolites from a microbial sample, such as a biofilm or agar culture; the metabolites are then replica "stamped" onto the NIMS surface. Using analytical standards we show that REX–NIMS effectively transfers and detects a range of small molecule compounds including amino acids and polyamines. This approach is then used to analyze the metabolite composition of streaked *Shewanella oneidensis* MR1 and *Pseudomonas stutzeri* RCH2 colonies and further resolve complex patterns produced by acoustic printing of liquid microbial cultures. Applying multivariate statistical analysis of the NIMS imaging data identified ions that were localized to different regions between and within colonies, as well as to the agar gel. Subsequent high-resolution tandem mass spectrometry was used to characterize two species-specific lipids that correlated with the spatial location of each microbial species and were found to be highly abundant in cell extracts. Overall, the use of acoustic printing of bacteria with REX–NIMS imaging will extend the range of analytical capabilities available for characterization of microbial interactions with mass spectrometry.

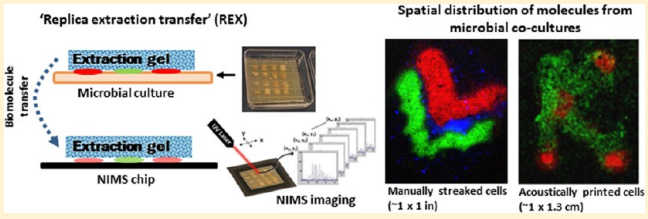

Microorganisms grow in complex microbial communities and possess a tremendous repertoire of metabolic and functional diversity.[1,2] However, traditionally studied as isolates in planktonic culture under controlled laboratory conditions, only a small fraction of these metabolic capabilities are actually expressed for subsequent analysis.[3] In the natural environment, microbes are often found populating complex, surface-attached communities (e.g., biofilms) that are exposed to and actively responding to a wide range of chemical and small molecule environments, as well as a multitude of other microbial species.[3] A required step toward actually understanding these naturally occurring community structures requires first the creation of simulated environments that can be used to interrogate the wide range of possible microbial interactions.

Acoustic printing presents an appealing approach for creating complex patterns of cells to examine microbial interactions. By using ultrasonic waves to eject liquid droplets from a multiwell plate, acoustic printing easily and rapidly transfers small volumes of liquid between plates or directly onto a solid surface; as a contact-free approach, this eliminates cross-contamination, carryover, and other technical problems encountered with precise transfer of small liquid volumes.[4] Currently, acoustic printing has found wide utility by the pharmaceutical industry for compound library management and high-throughput sample processing;[4] in mass spectrometry, it has also been used for printing trypsin onto tissues for MALDI imaging, reducing sample spot size in MALDI-MS for high-throughput, and enzyme reactions on NIMS surfaces.[5−7] More recently, acoustic transfer has found utility in bioprinting, in which living cells (and other biomolecules) are dispensed for such applications as spatial patterning for tissue engineering, cryopreservation, and other cell-based assays.[8−11] Taking advantage of these characteristics, here this technique is used to print multiple microbial species in spatially complex arrays

Received: July 20, 2013
Accepted: October 10, 2013
Published: October 10, 2013

onto agar plates; growth of these surface-attached colonies are used to serve as experimental recreations of naturally occurring environments.

To understand the chemical environment of microbial communities, it is important to directly probe the molecular composition as it occurs in situ to preserve endogenous spatial relationships. Mass spectrometry imaging (MSI) has enabled the label-free interrogation of metabolites directly within complex biological matrices, over a broad range of biological and nonbiological compounds (e.g., drugs, lipids, metabolites, peptides, etc.).[12] However, unlike metabolomics or proteomics of bulk extracts, in which the average molecular composition is determined for a sample, MSI creates a spatially defined map of molecular composition that includes the relative abundance of each molecule across the entire sample surface. A typical MSI experiment involves rastering a mode of desorption/ionization (D/I) (e.g., laser) sequentially across a sample while recording a mass spectrum at each point. One of the most common applications of MSI is imaging thin tissue sections, with results invaluable for determining whether changes are uniform throughout a tissue or localized to specific regions (a feature proven important in cancer biology and characterization of heterogeneous tumors), especially when used to complement other imaging and analytical approaches.[13,14,19,20] Imaging of bacterial colonies directly on agar gels has recently been accomplished with matrix-assisted laser desorption ionization (MALDI) and electrospray ionization (ESI)-based techniques.[15,16] In MALDI imaging, colonies grown on thin agar gels are dried onto an LDI plate, then subsequently treated with MALDI matrix and directly imaged.[17] Using desorption electrospray ionization (DESI), metabolite imaging in bacterial colonies involves scanning the surface with the ESI cone; using nano-DESI, a solvent bridge is created between two capillaries that is scanned over the surface.[18,19] Given the significant interest in microbial MSI, it would be desirable to extend other mass spectrometry approaches to this important application.

Nanostructure-initiator mass spectrometry (NIMS), for instance, is one such technique that has been developed that has significant advantages for metabolite imaging of small compounds (~1000 Da), does not use MALDI matrix (thereby avoiding matrix background ions and other matrix-related effects), and has high sensitivity and low background;[20] NIMS has also already been demonstrated for imaging tissue sections and microbial analysis of sample extracts.[14,21,22] However, because NIMS and related techniques generate gas phase ions from the surface−sample interface, mass spectrometry imaging has been limited to sections (of tissue or agar) sufficiently thin to transmit laser light to the surface (typically 5 μm or less). Consequently, technical challenges such as thin-sectioning frozen agar have thus far precluded NIMS imaging of microbial colonies.

Here, we address this issue and describe a novel technical platform for constructing complex arrangements of colonies using acoustic printing and a new "replica-extraction-transfer" (REX) technique to enable NIMS imaging of microbes grown on agar surfaces. REX was designed by analogy to conventional liquid−liquid extraction methods, in which liquid solvents are used to remove molecules from a homogenized sample matrix. However, in the present study, solvent-soaked gels are used to extract spatially defined metabolites from colonies and then transfer them onto the NIMS surface for subsequent mass spectrometry imaging. In principle, this approach is analogous to liquid−liquid extraction used for LC/MS and GC/MS-based metabolomics and has the potential that different molecule types can be targeted for imaging on the basis of solvent partition coefficients. We also demonstrate the use of contact-free acoustic printing to construct complex patterns of colonies on agar for extraction transfer imaging. Together, this provides a new platform for analysis of microbial growth and interactions on solid supports and customized biofilm growth, and the technique has the potential for enabling multimodal imaging by using direct (e.g., fluorescence) imaging of the colonies prior to or after mass spectrometry imaging.

EXPERIMENTAL SECTION

Chemicals and Microbial Cultures. Chemicals used in this study included ethanol (Sigma), chloroform (Sigma), hydrofluoric acid (Fisher), LC/MS water (Fluka), agarose (Sigma), agar (Alfa Aesar), and Luria−Bertani (LB) Miller broth (Amresco). Strains used in this study were *Shewanella oneidensis* MR1 (ATCC Cat. No. 700550) and *Pseudomonas stutzeri* RCH2 (a strain isolated from Cr(VI)-contaminated groundwater from Hanford 100H, WA, with acetate as the sole electron donor and nitrate as the sole electron acceptor[23]). These strains were cultured in liquid LB media or LB agar plates (solidified with 1.5−2% agar) from frozen glycerol stocks at 30 °C.

Acoustic Printing of Bacteria and Biomolecular Compounds. Acoustic printing was performed as described previously,[7] but in this work, samples were composed of liquid microbial culture. Briefly, by using an ATS-100 Acoustic Liquid Dispenser (EDC Biosystems, Fremont, CA), microbes in liquid media were printed from an acoustic 384-well plate in 10 nL droplets onto a target substrate (e.g., solidified LB agar media). Bacteria were printed in a variety of patterns with a microarray spot pitch (center-to-center distance) of 450 μm (template is shown in Figure S-2). Density of bacteria deposited in a particular location could be controlled by measuring the optical density (e.g., 600 nm) of liquid culture prior to printing, sample dilution, and printing one or more droplets in the same target location.

Replica Extraction Transfer Stamping Protocol for NIMS Imaging. Below, the protocol for extraction gel preparation (1), microbial sample preparation (2), and replica extraction transfer stamping (3) are described. (1) A 4% agarose gel was prepared by heating and dissolving agarose in Milli-Q water and then pouring it as a thin layer (~4−8 mm) into a sterile Petri dish and solidifying at room temperature. (2) Microbial cultures were grown on agar media for specified time periods. To prepare the samples for imaging, a section of the microbial culture on agar was carefully excised, placed face-up on a glass slide (positively charged), and dried at 35 °C in a food dehydrator (FD-61 Snackmaster, NESCO/American Harvest, Two Rivers, WI) for ~1−2 h. As an alternative to excising agar pieces, the entire culture on agar was dried in situ in the Petri dish. (3) A section of extraction gel was excised and soaked in extraction solvent (100% MeOH, 1:1 MeOH/H_2O, 100% H_2O, etc.) for 10−30 min. The gel was then removed, and excess solvent was drained. The upper surface of the extraction gel was then placed onto the dried microbial culture for ~30 s (slight pressure was applied to ensure complete contact and expulsion of bubbles) and then removed. Extracted biomolecules were then immediately transferred (stamped) onto the NIMS chip surface by contacting the upper extraction gel surface to the NIMS chip surface for ~10 s and then removing the gel.

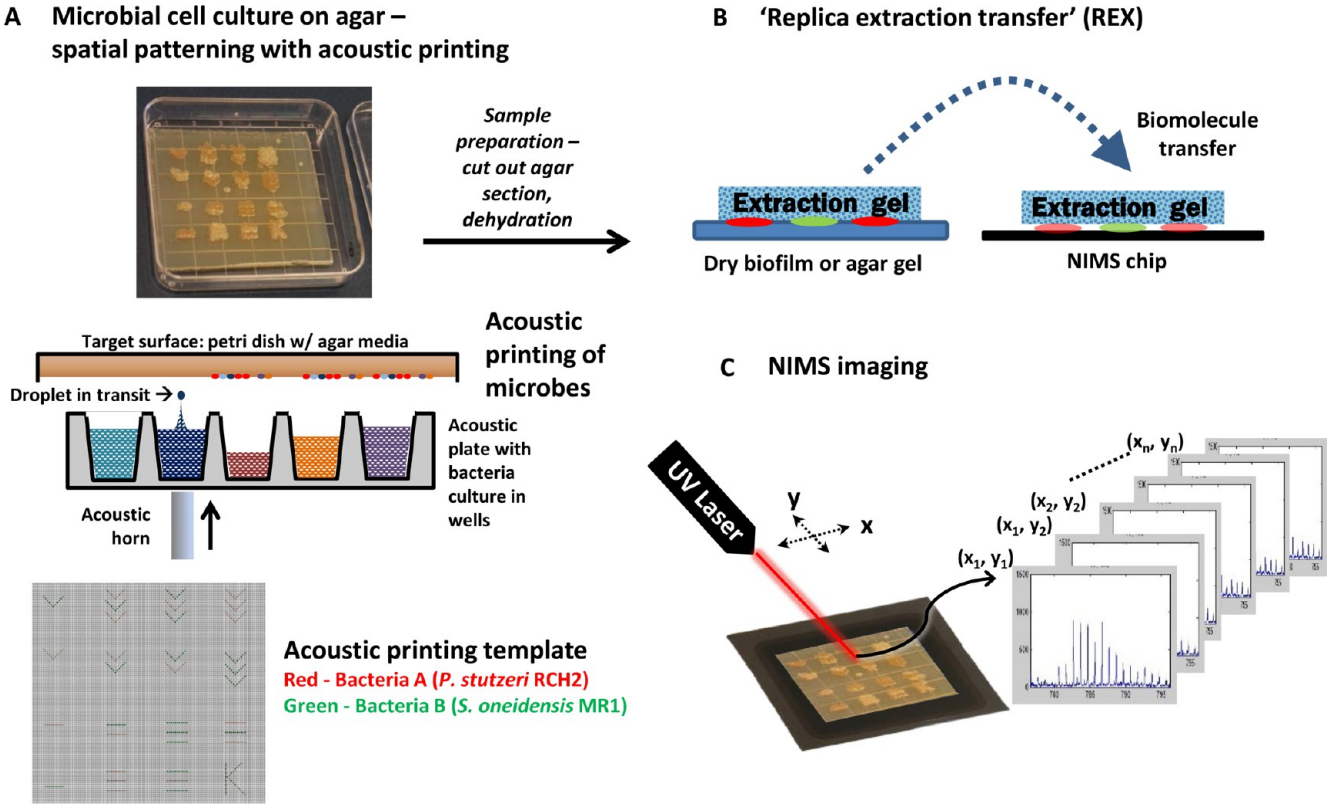

Figure 1. Workflow for "replica-extraction-transfer" (REX) NIMS imaging. (A) Microbes are grown on agar media or other surface. For spatial patterning with acoustic printing, 1−10 nL droplets of microbes in liquid media are acoustically printed onto an agar surface according to a predetermined custom template. (B) In preparation for REX, the biofilm or agar gel with cultured microbes is first dehydrated. For biomolecule extraction, a solvent-laden gel is placed upon the dried microbial surface with slight pressure; for biomolecule transfer, the gel is removed, then the same side is contacted to a NIMS chip surface. (C) For NIMS imaging, a laser is rastered across the spatially transferred biomolecules to generate an individual mass spectrum at each position.

NIMS Wafer Fabrication. Preparation of a NIMS surface has been thoroughly described elsewhere.[24,25] Briefly, silicon wafers (Silicon Quest International, Santa Clara, CA) (single-sided polished P/Boron, orientation <1 0 0 >, resistivity 0.01−0.02 Ω cm, 525 ± 25 μm thick) were electrochemically etched using 25% hydrofluoric acid in ethanol under a constant current of 2.4 A for 15 min, and they were then coated with bis(heptadecafluoro-1,1,2,2-tetrahydrodecyl) tetramethyl-disiloxane (Gelest, Morrisville, PA) as an initiator.

NIMS Imaging of Spatially Extracted Metabolites. A NIMS chip with extracted/transferred metabolites were imaged using a 4800 or 5800 MALDI TOF/TOF (AbSciex, Foster City, CA) in positive reflector MS mode with an Nd:YAG laser (200 Hz, 2500−4200 laser intensity) acquiring spectra over a range of 20−1500 Da (700−900 Da focus mass) and accumulating 18 shots/spot. The 4800 Imaging Tool software (Novartis and Applied Biosystems) was used to raster across the sample and record spectra in *x*-*y* step-sizes ranging from 50 × 50 to 100 × 100 μm. Data viewing and image reconstruction were performed using custom software developed in-house using the Matlab (Mathworks, Natick, MA) programming language and OpenMSI (https://openmsi.nersc.gov).

Metabolite Extraction from Homogenized Microbial Cultures. Cell extractions were performed on monocultures and cocultures of *P. stutzeri* RCH2 and *S. oneidensis* MR1 grown on LB agar plates and in LB liquid media. Both washed and unwashed cells were extracted in two different solvent systems: (1) 100% MeOH, the same solvent used for REX-MSI of microbial cultures and (2) a chloroform-based extraction. For the 100% MeOH extraction, cells were dried and resuspended in 100% MeOH, and then cell disruption was performed via a 15 s ultrasonic pulse (125 W, 20 kHz, 40% amplitude, CL-18 probe; Qsonica, Newtown, CT), followed by a 30 min incubation in a sonic water bath (Symphony; VWR, Radnor, PA) at 30 °C. The supernatant was collected following centrifugation. A chloroform-based extraction was also performed to enrich the nonpolar component of the extract to generate higher signal intensities in spotted extracts required for subsequent MS/MS analysis. Here, a Bligh−Dyer approach was used to extract lipids and other nonpolar compounds from the chloroform phase in a 1:1:1 chloroform/MeOH/H_2O solvent system.[26] Sample extracts were dried, redissolved in 100% MeOH or chloroform, and spotted directly onto a NIMS chip in 0.5 μL droplets. Mass spectra were obtained using two instruments: (1) 5800 TOF/TOF (AbSciex, Foster City, CA) in positive reflector MS mode with an Nd:YAG laser (200 Hz), acquiring over a range of 20−1500 Da (900 Da focus mass) and accumulating 18 shots/spot and (2) MALDI LTQ Orbitrap (Thermo Scientific, Waltham, MA) in positive mode, acquiring full range MS spectra as well as MS2 via collision-induced dissociation (CID) and higher energy collision dissociation (HCD) on selected ions.

Light Microscopy Imaging. A light microscopy image (M165 FC; Leica Microsystems, Wetzlar, Germany) or photo was taken of each sample prior to or after dehydration and REX

dx.doi.org/10.1021/ac402240q | *Anal. Chem.* 2013, 85, 10856−10862

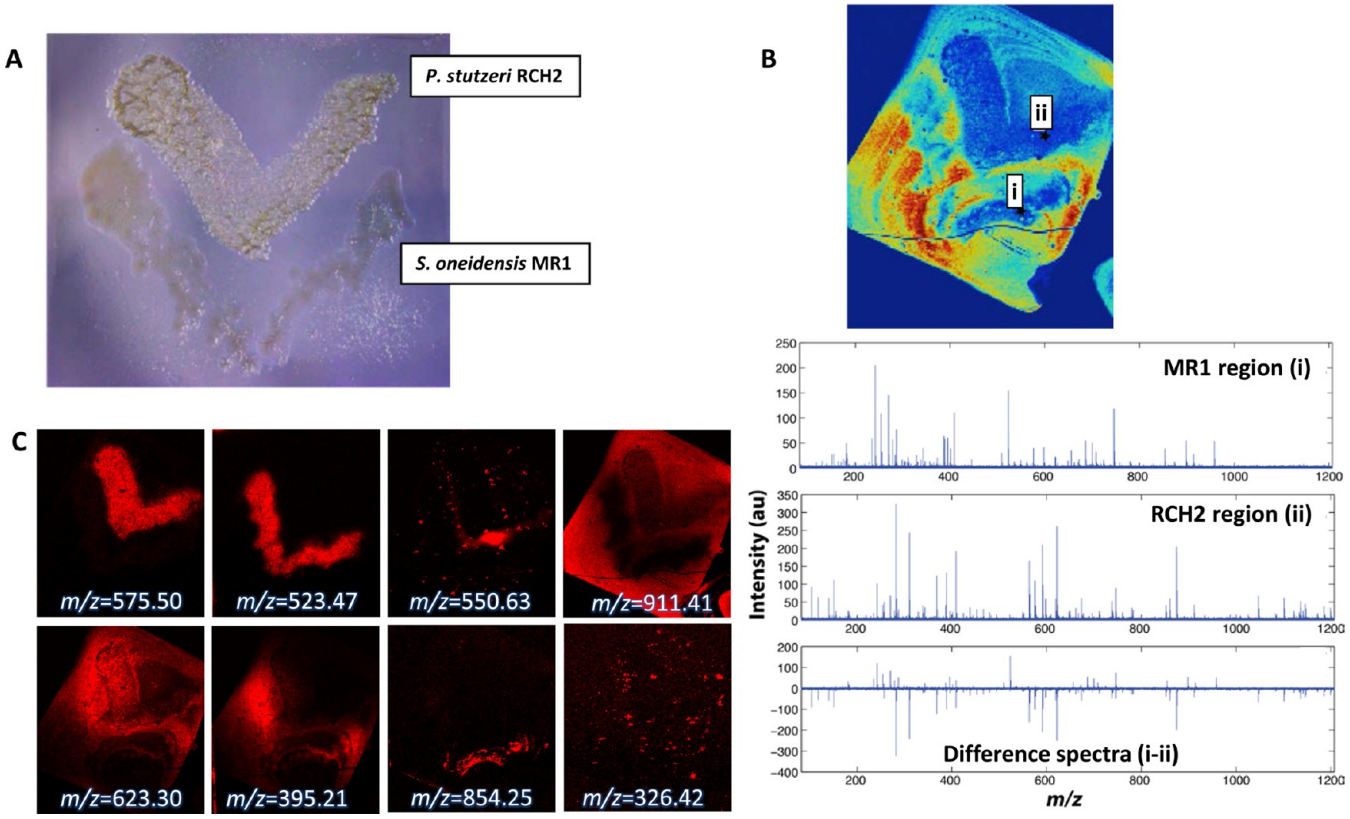

Figure 2. REX–NIMS imaging of a microbial culture grown on LB agar. (A) Stereoscope image of a multispecies interaction between *P. stutzeri* (top V) and *S. oneidensis* (bottom V) streaked in a double-V (≪) pattern. (~1 in. x 1in) (B) Different spectra observed between representative pixels from RCH2 vs MR1 regions. (i) single pixel spectra from *S. oneidensis* MR1 region (ii) single pixel spectra from *P. stutzeri* RCH2 region (i-ii) difference spectra (C) Single ion images of heterogeneously distributed biomolecules using REX–NIMS imaging protocol.

to correlate microbial spatial relationships with the resulting mass spectrometry images.

Mass Spectrometry Imaging Data Processing. Raw spectra were imported from each image file (.img format). All raw MS imaging spectra were corrected in mass to match two corresponding m/z values detected in the high mass accuracy Thermo Orbitrap of spotted extracts. Pixels comprising the mass spectrometry image were grouped into two regions by *K*-means analysis using a correlation distance function in Matlab 2011b,[27] followed by the nonbackground region being grouped into six further subregions. This identified and grouped pixels with similar spectral patterns on the basis of similar relative intensities for the detected ions.

RESULTS AND DISCUSSION

REX–NIMS Imaging Technique. Sample preparation is often a major technical challenge in mass spectrometry imaging, particularly in the study of spatially organized microbial communities in which proteins, salts, etc. from agar plates may significantly reduce or suppress signal from the target analyte. Surface roughness may also negatively influence the mass resolution detected across a sample as the time-of-flight for a molecules varies with sample thickness. Here, we describe a new technique for transferring biomolecules from a microbial sample onto a NIMS silicon surface that can be directly used for imaging. This "replica-extraction-transfer" technique (REX) for mass spectrometry imaging was designed by analogy to conventional liquid–liquid extraction methods in which liquid solvents are used to remove molecules from a homogenized sample matrix. In contrast, REX is performed in situ on a nonhomogenized microbial culture by using a solvent-soaked gel to preserve the spatial relationships of biomolecules during transfer (Figure 1).

An overview of the REX–NIMS imaging workflow is outlined in Figure 1. Here we focus on microbial culture on agar. However, it is likely that this approach can be used for a variety of other applications/surfaces (e.g., biofilm, soil, rock) (Figure 1A). To prepare for extraction, samples are first dried, and then a gel soaked in extraction solvent is used to transfer biomolecules from the sample surface to the NIMS chip surface (Figure 1B). NIMS imaging is then performed on the spatially transferred biomolecules using a MALDI-TOF instrument to generate a spectrum at each location (Figure 1C). Spectra are analyzed in mass spectrometry imaging software to generate single ion images that spatially map individual molecules, as well as other types of imaging analysis.

Replica Extraction Transfer of Metabolite Standards. Analytical standards were used to examine the ability to transfer molecules within a dried agar gel to a NIMS imaging surface. Given the difficulty in detecting very small metabolites using MALDI-MSI we selected molecules in the 100–300 Da range. Individual pieces of agar were individually soaked in concentrated solutions (Table S-1) for ~1 h to allow time for biomolecules to diffuse into the gel. Excess solvent was removed and these soaked pieces were dehydrated on a glass slide in a grid pattern. REX was performed using 1:1 MeOH:H_2O to extract and transfer the grid onto the NIMS chip (Figure S-1). Adenosine, 4-pyrrolidinopyridine, ectoine, proline, sperimine, spermidine, tryptophan, methionine, lysine

dx.doi.org/10.1021/ac402240q | *Anal. Chem.* 2013, 85, 10856–10862

and leucine were all easily detected. Not surprisingly, cations (e.g., ectoine) and strongly cation forming metabolites had the highest intensity (e.g., spermine, spermidine) in positive mode; in contrast, weakly cation forming metabolites were barely detected (valine, aspartate, glutamate). Relative ion intensity and spectra for detected compounds can be found in Figure S-2.

While this particular experiment demonstrated the utility of REX in mass spectrometry imaging of small molecules, only a single extraction solvent was employed. Similar to bulk extraction of homogenized samples, it is expected that different solvent systems (e.g., butanol, H_2O, MeOH, MeOH/H_2O) may extract a different molecular profile from the same sample (lipids versus hydrophilic amino acids, basic versus acidic, hydrophobic versus hydrophilic molecules, etc).

REX−NIMS Imaging of Microbial Cultures Enables Visualization of Spatial Heterogeneity in Coculture and Defines Microbe-Specific Ions. To determine whether REX could be used for mass spectrometry imaging of microbial cultures we first tested the approach with simple patterns from streaked cultures. Here, we prepared mono- and cocultures of *P. stutzeri* and *S. oneidensis* on LB agar media. These two bacteria were selected because they are easily distinguished based on morphology when grown on LB agar (*S. oneidensis* = red/flat; *P. stutzeri* = white/wrinkled); additionally, they are both capable of reducing Cr(VI), a property desirable for bioremediation in groundwater contamination (e.g., Hanford).[23,28] Figure 2 shows an example in which these two microbes were streaked in a double V pattern (≪), providing fiduciary markers of top microbe vs bottom microbe), cultured 4 days, then dried and imaged using REX−NIMS with an agarose transfer gel soaked in 100% MeOH. Spectra from the resulting mass spectrometry images using REX−NIMS analysis showed a spatial distribution of molecules that correlated with light microscopy images showing where each microbe was initially plated and growing (Figure 2A,B).

The spatial heterogeneity of the microbial coculture was then visualized by applying K-means analysis between the MSI spectra comprising each pixel (Figure S-3). Briefly, spectrally similar pixels were clustered into 2 groups to separate background (A) from biologically relevant pixels (B), which could be confirmed visually (based on microbe color) as well as by spectral pattern. Pixels comprising the biologically relevant group (B) were further subdivided into 6 groups that were spectrally similar (B1−B6). Here, we find that spectra comprising regions B3 and B5 correspond to the spatial location of visually observable growth of *P. stutzeri* or *S. oneidensis* colonies, respectively.

Next, to find biomolecules that could be used to differentiate the spatial locations of different microbial species, spectra from individual pixels located in K-means regions B3 and B5 were compared. As shown in Figure 2B, the spectra from a pixel located in a *P. stutzeri* region (ii) shows a different distribution of detected molecules than the spectra from a pixel located in an *S. oneidensis* region (i). These differences were also apparent in homogenized extracts of *P. stutzeri* and *S. oneidensis* colonies grown on agar (Figure S-4A,B). Here, since the REX image is a form of extraction, we observed many of the same ion m/z values in both the spotted cell extracts as well as imaging data. This is in contrast to typical mass spectrometry imaging data in which the sample is not extracted but directly imaged. In these, strong biological matrix effects typically result in formation of different ions with in situ direct imaging vs corresponding extracts.[29] For example, $[M+K]^+$ or $[M+Na]^+$ ions are typically detected in direct imaging experiments of tissue using NIMS, whereas corresponding $[M+H]^+$ adducts will be detected in extracts of the same sample.[22] Observing primarily $[M+H]^+$ adducts in both the extract and image is extremely advantageous in sample analysis for many reasons. For instance, it is difficult to determine whether the detected abundance of a particular biomolecule distributed across a sample is a result of K^+ vs Na^+ abundance in different locations in the biospecimen (influencing a molecule's ionization properties) or true biomolecule abundance. Also, this eliminates the need to correlate differing m/z values (based on adduct) for the same biomolecule between the extract and imaging spectra.

The observed differences in metabolite composition spanned the mass range (50−1500 m/z). In this work, a metabolite is defined as an intermediate or product of metabolism, and within the context of metabolomics, as a molecule <1000 Da in size.[30] Table S-2 lists some of the biomolecules that differentiated *P. stutzeri* from *S. oneidensis*. While identification of each of these compounds would be interesting, it is beyond the scope of this work; however, here we provide information (m/z values and spatial distribution for each microbial species) for guiding later identification from, for instance, a spectral library of identified microbial compounds.[31] Here, we narrowed the scope of identification to focus on two highly abundant metabolites observed in both the cell extracts and imaging data: m/z = 575.50 and m/z = 523.47, respectively. As shown in single ion images, m/z = 575.50 and 523.47 spatially correlated with either *P. stutzeri* or *S. oneidensis* (Figure 2C). MS spectra from corresponding cell extractions showed these ions to be highly abundant in the corresponding species, as shown in representative spectra in Figure S-4A,B. To confirm that these ions were from cells and not media, and that these molecules are soluble in both a 100% MeOH and chloroform-extracted system, washed and unwashed cell samples were extracted in both solvent systems and found to be present in all extracts. Together, this provided confirmation of the microbe-specificity of these m/z values.

High resolution CID and HCD MS/MS (Figure S-4C−H) suggest that a lipid species, putatively identified as a menaquinone (m/z 523.47), is localized to *S. oneidensis*, which is consistent with previous reports.[32] By comparing HCD MS/MS fragmentation spectra between m/z = 523.47 (MR1) with m/z = 575.50 (RCH2) (Figure S-4G,H), both molecules appear to have some structural similarity. Both biomolecules (based on exact mass) share the same C5 to C8 unsaturated hydrocarbon fragments (w/2 double bonds as the dominant fragment − red outline);[33] the dominant C9 and C10 hydrocarbon fragments between these molecules differ by 1 double bond (dark and light blue outline).

Many ions were found to be heterogeneously distributed in the agar surrounding the colonies and therefore could be indicative of metabolic processes not easily apparent when visualized by light microscopy. A representative sample of these molecules is shown as single ion images in Figure 2C. Some of these showed spatial distributions that could be inferred as arising from LB agar molecules (e.g., m/z = 911.4), with higher intensity values at the perimeter of the gel and lower values closer to the microbes; this suggests metabolic uptake of these by the growing microbes. Some ions appeared to be higher intensity around the perimeter of each microbe, suggesting anabolic production or perhaps secretion from either *P. stutzeri* (e.g., m/z = 623.3) or *S. oneidensis* (e.g., m/z = 395.2). Further,

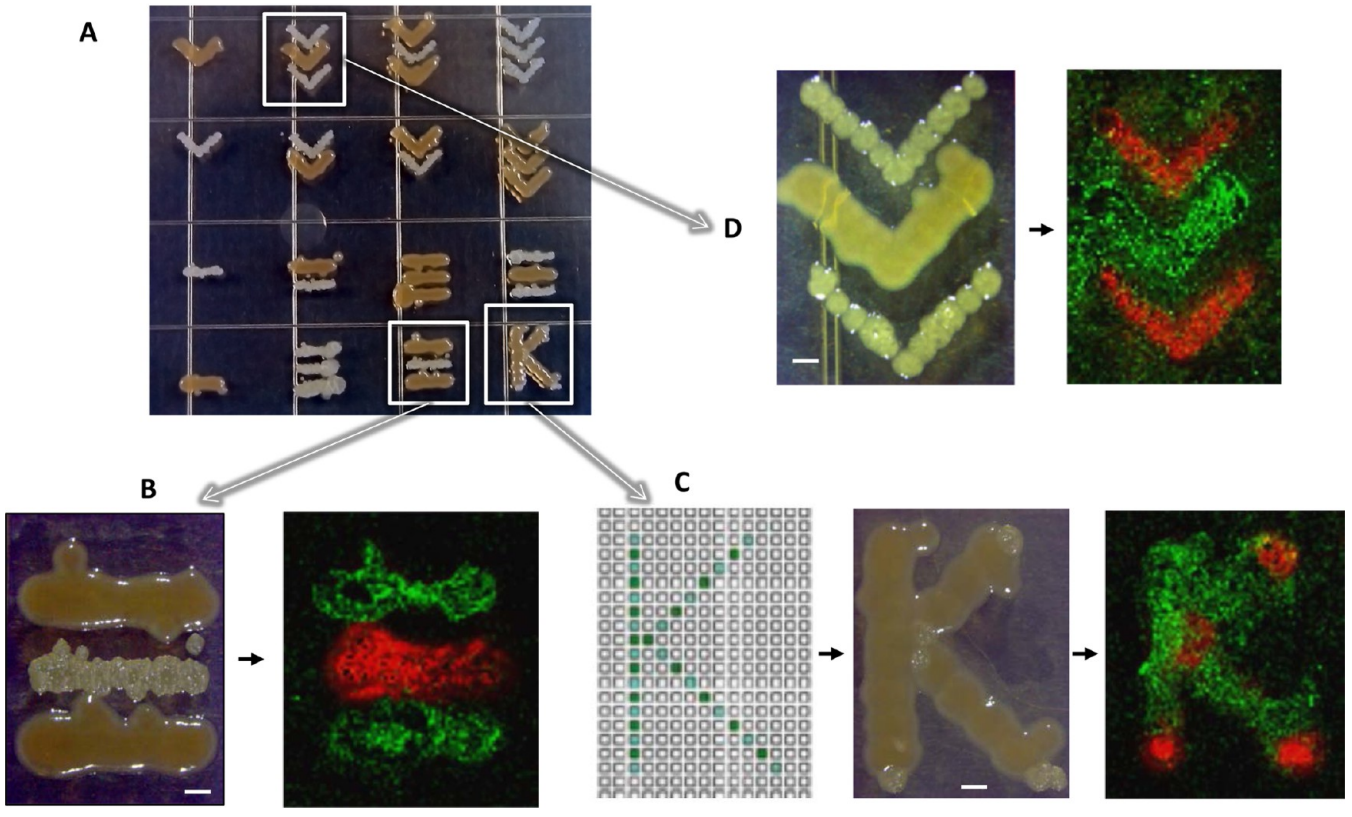

Figure 3. Acoustic printing of cells create high-resolution complex spatial patterns. (A) Image of two different microbial species (*P. stutzeri* and *S. oneidensis*) acoustically printed onto LB agar at a 450 μm center-to-center distance, then grown 24 h. (B) Light microscope image of microbes grown in "lines" pattern with corresponding ion image (red:m/z = 575.5; green:m/z = 700.2). (C) Acoustic printing template and light microscope image of microbes grown in "K" pattern with corresponding ion image (red:m/z = 74.2; green:m/z = 700.2). (D) Light microscope image of microbes grown in "≪" pattern with corresponding ion image (red:m/z = 74.2; green:m/z = 700.2). Petri dish grid = 2 cm ×2 cm/square; scalebar =1 mm.

some ions were intense primarily within an area directly between the V's; these may be associated with interactions and/or communication between the two microbial species (e.g., m/z = 550.6). However, it is interesting to note that in the image, the molecules detected in this area do not span the complete area between the colonies. This may be related to lack of symmetry when colonies were streaked as well as uneven growth. In addition, some ions had a spatial distribution with a "speckling" pattern across the image (e.g., m/z = 326.4), whereas others were distributed along only the outer edge of *S. oneidensis* (e.g., m/z = 854.25). A broader sampling of observed m/z values are provided in Table S-2 and corresponding single ion images in Figure S-5.

Acoustic Printing of Cells To Create Complex Spatial Patterns of Bacteria. Here, an acoustic liquid transfer system is used to print droplets of microbes in liquid media in spatially complex patterns at high spatial resolution, printing droplets from a source plate to an inverted agar gel target (Figure 1A). To test and develop acoustic printing for creating complex spatial patterns of these two different microbial species, templates were constructed using three geometries: V's, 'lines', and K's. For V's and 'lines', each V or 'line' was comprised of only a single microbial species with droplets printed 450 μm center-to-center grid. In contrast, the K's were printed with alternating droplets of *S. oneidensis* and *P. stutzeri*. The acoustic template implemented is shown in Figure S-2A (green = *S. oneidensis* droplet; red = *P. stutzeri* droplet), with a corresponding movie of the actual printing process provided in Movie S-1. A total of 4 replicate plates were printed with each plate taking ∼1 min to print in entirety.

As shown in Figure S-6B, the droplet locations are only barely visible to the naked eye directly after printing. After 1 and 3 days of culture, the growth of bacteria is clearly in the same pattern as that of the custom-designed acoustic template, reflecting the high fidelity and reproducibility of the technique (Figure 3). In particular, the *P. stutzeri* (Figure 3D) shows equal spacing and linear arrangement. In some cases, 'satellite' spots are detected (Figure 3B), which is attributed to spattering during the printing process. Although not optimized for printing cells, follow-up experiments using pure liquids suggest this effect may be minimized by printing smaller droplets of pure liquids, and this represents a promising future direction for using the facile acoustic printing of replicate culture and avoiding these confounding experimental effects.

REX−NIMS Imaging of Acoustically Printed Bacteria. After 1 day of culturing, the spatial location of each microbial species is easily visualized based on the color of the two microbes (Figure 3). However, after 3 days of culturing, the interactions between the species make differentiating the spatial location of the two species more difficult (Figure S-6B-iii). Here, we compared microscope images with subsequent REX−NIMS to determine the spatial fidelity of REX−NIMS. For these samples, REX−NIMS preserved the relative arrangement of the two microbes. As can be observed in Figure 3D, the round colony features in the RCH2 "Vs" observed in the microscopy images are also apparent in the REX−NIMS images. From this we estimate a resolution of approximately

dx.doi.org/10.1021/ac402240q | *Anal. Chem.* 2013, 85, 10856−10862

150 μm, suggesting that REX is a minimal perturbation of the natural spatial locations at this scale.

In the case of the printed "K," which alternated between printing *S. oneidensis* and *P. stutzeri* every 450 μm, there is a spatial correspondence between the visual location of the 2 different microbial species in the optical image and the ions used to make the image (notated in the figure caption for each). It is interesting to note that in this spatial patterning, *P. stutzeri* is only observed in the center and edges of the "K" pattern, suggesting that *S. oneidensis* may outcompete *P. stutzeri* lacking sufficient cell density or open access to nutrients.

CONCLUSION

In this work, we describe acoustic printing of bacteria coupled with "replica-extraction-transfer" NIMS imaging. Using analytical standards, we show that REX–NIMS is capable of detecting a range of small molecules from agar gels. Acoustic printing is described for patterning arrays of cells and constructing complex spatial patterns of two bacterial species (*S. oneidensis* and *P. stutzeri*) for REX–NIMS experiments. Comparison of REX–NIMS and microscope images confirms that this approach is capable of generating spatially preserved chemical images that distinguish chemically distinct regions in a microbial culture. Future work will focus on improving the spatial resolution of this approach and application toward the study of specific, defined microbial interactions.

ASSOCIATED CONTENT

Supporting Information

Further information can be found in separate files: Figures S-1–4,6, Tables S-1–2, Movie S-1, and Figure S-5. This material is available free of charge via the Internet at http://pubs.acs.org.

AUTHOR INFORMATION

Corresponding Author

*E-mail: trnorthen@lbl.gov.

Author Contributions

T.N., B.B., and K.L. provided conception and overall experimental design, analyzed data, and wrote the manuscript. K.L., J.B., B.B., and X.C. designed and performed experiments and contributed to manuscript editing. A.A., A.D., R.C., and J.B. advised on cell culture, experimental design and applicability to microbiology, and contributed to manuscript editing.

Notes

The authors declare no competing financial interest.

ACKNOWLEDGMENTS

This work was conducted by ENIGMA—Ecosystems and Networks Integrated with Genes and Molecular Assemblies Program—from the Office of Biological and Environmental Research of the U.S. Department of Energy as supported by the Office of Science, Office of Biological and Environmental Research, U.S. Department of Energy, under Contract No. DE-AC02-05CH11231. We would like to thank G. Karpen and R. Baran for valuable discussions and guidance and Z. Baliga for assistance with microbial photography. Special thanks to M. Prieto Conway and Thermo Fischer Scientific for assistance in acquiring MS and MS/MS data and Professor V. Shulaev for generously providing access to his laboratory equipment.

REFERENCES

(1) Berleman, J. E.; Kirby, J. R. *J. Bacteriol.* **2007**, *189*, 5675–5682.
(2) Kearns, D. B.; Losick, R. *Mol. Microbiol.* **2003**, *49*, 581–590.
(3) Kolenbrander, P. E.; Palmer, R. J., Jr.; Periasamy, S.; Jakubovics, N. S. *Nat. Rev. Microbiol.* **2010**, *8*, 471–480.
(4) Zaragoza-Sundqvist, M.; Eriksson, H.; Rohman, M.; Greasley, P. J. *J. Biomol. Screening* **2009**, *14*, 509–514.
(5) Tu, T.; Gross, M. L. *TrAC, Trends Anal. Chem.* **2009**, *28*, 833–841.
(6) Aerni, H. R.; Cornett, D. S.; Caprioli, R. M. *Anal. Chem.* **2006**, *78*, 827–834.
(7) Greving, M.; Cheng, X.; Reindl, W.; Bowen, B.; Deng, K.; Louie, K.; Nyman, M.; Cohen, J.; Singh, A.; Simmons, B.; Adams, P.; Siuzdak, G.; Northen, T. *Anal. Bioanal. Chem.* **2012**, *403*, 707–711.
(8) Zhang, X.; Khimji, I.; Shao, L.; Safaee, H.; Desai, K.; Keles, H. O.; Gurkan, U. A.; Kayaalp, E.; Nureddin, A.; Anchan, R. M.; Maas, R. L.; Demirci, U. *Nanomedicine* **2012**, *7*, 553–564.
(9) Fang, Y.; Frampton, J. P.; Raghavan, S.; Sabahi-Kaviani, R.; Luker, G.; Deng, C. X.; Takayama, S. *Tissue Eng., Part C* **2012**, *18*, 647–657.
(10) Tasoglu, S.; Demirci, U. *Trends Biotechnol.* **2013**, *31*, 10–19.
(11) Durmus, N. G.; Tasoglu, S.; Demirci, U. *Nat. Mater.* **2013**, *12*, 478–479.
(12) Chaurand, P.; Schwartz, S. A.; Reyzer, M. L.; Caprioli, R. M. *Toxicol. Pathol.* **2005**, *33*, 92–101.
(13) Deutskens, F.; Yang, J.; Caprioli, R. M. *J. Mass Spectrom.* **2011**, *46*, 568–571.
(14) Louie, K. B.; Bowen, B. P.; McAlhany, S.; Huang, Y. R.; Price, J. C.; Mao, J. H.; Hellerstein, M.; Northen, T. R. *Sci. Rep. (U.K.)* **2013**, 3.
(15) Schwamborn, K.; Caprioli, R. M. *Mol. Oncol.* **2010**, *4*, 529–538.
(16) Yang, J. Y.; Phelan, V. V.; Simkovsky, R.; Watrous, J. D.; Trial, R. M.; Fleming, T. C.; Wenter, R.; Moore, B. S.; Golden, S. S.; Pogliano, K.; Dorrestein, P. C. *J. Bacteriol.* **2012**, *194*, 6023–6028.
(17) Watrous, J. D.; Dorrestein, P. C. *Nat. Rev. Microbiol.* **2011**, *9*, 683–694.
(18) Wu, C.; Dill, A. L.; Eberlin, L. S.; Cooks, R. G.; Ifa, D. R. *Mass Spectrom. Rev.* **2012**, *32*, 218–243.
(19) Watrous, J.; Hendricks, N.; Meehan, M.; Dorrestein, P. C. *Anal. Chem.* **2010**, *82*, 1598–1600.
(20) Stolee, J. A.; Walker, B. N.; Zorba, V.; Russo, R. E.; Vertes, A. *Phys. Chem. Chem. Phys.* **2012**, *14*, 8453–8471.
(21) Walker, B. N.; Antonakos, C.; Retterer, S. T.; Vertes, A. *Angew. Chem., Int. Ed.* **2013**, *52*, 3650–3653.
(22) Lee do, Y.; Platt, V.; Bowen, B.; Louie, K.; Canaria, C. A.; McMurray, C. T.; Northen, T. *Integr. Biol.* **2012**, *4*, 693–699.
(23) Han, R.; Geller, J. T.; Yang, L.; Brodie, E. L.; Chakraborty, R.; Larsen, J. T.; Beller, H. R. *Environ. Sci. Technol.* **2010**, *44*, 7491–7497.
(24) Reindl, W.; Bowen, B. P.; Balamotis, M. A.; Green, J. E.; Northen, T. R. *Integr. Biol.* **2011**, *3*, 460–467.
(25) Woo, H. K.; Northen, T. R.; Yanes, O.; Siuzdak, G. *Nat. Protoc.* **2008**, *3*, 1341–1349.
(26) Bligh, E. G.; Dyer, W. J. *Can. J. Biochem. Physiol.* **1959**, *37*, 911–917.
(27) Jones, E. A.; van Remoortere, A.; van Zeijl, R. J.; Hogendoorn, P. C.; Bovee, J. V.; Deelder, A. M.; McDonnell, L. A. *PLoS One* **2011**, *6*, e24913.
(28) Myers, C. R.; Carstens, B. P.; Antholine, W. E.; Myers, J. M. *J. Appl. Microbiol.* **2000**, *88*, 98–106.
(29) Murphy, R. C.; Hankin, J. A.; Barkley, R. M. *J. Lipid Res.* **2009**, *50* (Suppl), S317–S322.
(30) Samuelsson, L. M.; Larsson, D. G. *Mol. BioSyst.* **2008**, *4*, 974–979.
(31) Bowen, B. P.; Northen, T. R. *J. Am. Soc. Mass Spectrom.* **2010**, *21*, 1471–1476.
(32) Frolova, G. M.; Pavel, K. G.; Shparteeva, A. A.; Nedashkovskaia, O. I.; Gorshkova, N. M.; Ivanova, E. P.; Mikhailov, V. V. *Mikrobiologiia* **2005**, *74*, 766–771.
(33) Bowen, B. P.; Fischer, C. R.; Baran, R.; Banfield, J. F.; Northen, T. *BMC Genomics* **2011**, *12* (Suppl 1), S6.